

Giant optical vortex in photonic crystal waveguide with nonlinear optical cavityEvgeny N. Bulgakov^{1,2} and Almas F. Sadreev¹¹*L.V. Kirensky Institute of Physics, 660036, Krasnoyarsk, Russia*²*Sibian State Aerospace University, Krasnoyarsk, Russia*

(Received 23 December 2011; revised manuscript received 22 February 2012; published 9 April 2012)

We consider light transmission in a directional photonic crystal waveguide that holds a nonlinear defect with two resonant dipole modes within the light propagation band. For the defect positioned on the center line of the waveguide, there are two ways to break the mirror symmetry with respect to either light intensity or light phase. The latter results in a giant vortex of the Poynting vector of the power current within the defect exceeding the input current by, at least, two orders of magnitude. We also consider the breaking of symmetry relative to the mirror reflection with respect to the cross-sectional axis of the waveguide when light is injected equally into both ends of the waveguide. This leads to different light outputs determined by the vorticity of the optical vortex.

DOI: [10.1103/PhysRevB.85.165305](https://doi.org/10.1103/PhysRevB.85.165305)

PACS number(s): 42.25.Bs, 42.65.Pc, 42.70.Qs

I. INTRODUCTION

The phenomenon of symmetry breaking is studied around two decades in the nonlinear optics with the establishment of one or more asymmetric states that no longer preserve the symmetry properties of the original state for injection of input power.¹⁻⁶ That well correlates with studies in a nonlinear dual-core directional fiber,⁷⁻⁹ the nonlinear Schrödinger equation in double-well potential¹⁰ and a linear discrete chain (Schrödinger lattice) with two nonlinear sites.¹¹ In all cited papers, the symmetry was broken because of different light intensities at the cavities. In Ref. 12, it was found that the symmetry might be broken because of different phases of light oscillations in the nonlinear cavities that gives rise to a Josephson-like Poynting vector (PV) of power current between the cavities.

In the present paper, we consider symmetry breaking in the one-dimensional directional photonic crystal (PhC) waveguide that holds a single nonlinear defect positioned on the center line of the waveguide. When only the monopole eigenmode of the defect cavity belongs to the propagation band of PhC waveguide, there is a variety of nonlinear optical processes mostly related to a bistability of light transmission,¹³⁻¹⁷ however, there is no room for the breaking of symmetry. We open that room by consideration of two dipole resonant modes of the single nonlinear defect made from a Kerr medium. The degenerated dipole modes have opposite parities relative to injected even light mode propagating in the waveguide. As a result for the linear cavity, the light would be coupled with the even dipole mode only to give rise to Breit-Wigner resonant peak at the eigenfrequency of the cavity. However, nonlinear coupling between the dipole modes may cause excitation of both dipole modes. The principal question for that phenomenon is the difference between phases of mode excitations. For equal phases, the symmetry is broken by the light intensity relative to mirror reflection. We will show in this paper that the dipole modes might be excited with different phases. As a result, we obtain optical vortex for the PV as was first considered by Nye and Berry.¹⁸ A novelty of that result is the extremely large value of the power current circulating the interior of the cavity.

One of the most ambitious goals in nonlinear optics is the design of an all-optical computer that will overcome the

operation speeds in conventional (electronic) computers. Vital in this respect is the design of basic components such as all-optical routing switches and logic gates. It is believed that future integrated photonic circuits for ultrafast all-optical signal processing require different types of nonlinear functional elements such as switches, memory, and logic devices. Therefore both physics and designs of such all-optical devices have attracted significant research efforts during the last two decades, and most of these studies utilize the concepts of optical switching and bistability. The concept of the all-optical switching is based on a discontinuous transition between the symmetry breaking solutions by a small change of the input.^{19,20} Many of these devices employ a configuration of two parallel coupled nonlinear waveguides.²¹⁻²⁵ Recently, Maes *et al.* demonstrated the all-optical switching in the system of two nonlinear microcavities aligned along the single waveguide²⁶ by the use of pulses of injected light. In the T-shaped waveguide coupled with two nonlinear microcavities, it was shown that pulses of light injected into a bottom waveguide are capable to switch light outputs.²⁷ In the present paper, we find the domains of stability for the solutions of the nonlinear coupled-mode equations that can be the basis for the all-optical switching in the simplest PhC architecture of a single waveguide with a single nonlinear optical cavity.

II. COUPLED-MODE THEORY

The PhC waveguide is formed by removing of a single row of the dielectric rods as shown in Fig. 1. The waveguide supports a single band of guided TM mode spanning from the bottom band edge 0.315 to the upper one 0.41 in terms of $2\pi c/a$.²⁸ The TM mode has the electric field component parallel to the infinitely long rods. Light propagating in the waveguide can excite only those eigenmodes of the defect rod cavity whose eigenfrequencies belong to the propagation band of the PhC waveguide. By tuning of the radius of the defect rod or its dielectric constant, we fit the dipole eigenfrequencies into the propagation band of the waveguide.¹⁷ Two degenerated dipole modes $E_1(\mathbf{x})$ and $E_2(\mathbf{x})$ of the defect rod cavity are shown in Fig. 1 for the case of a closed defect. Then we open the defect removing the rods marked by dashed open

FIG. 1. (Color online) (a) Even and (b) odd eigendipole eigenmodes E_1 and E_2 , respectively, with the degenerated eigenfrequency $\omega_0 = 0.3763$ in the two-dimensional square lattice PhC consisted of the GaAs dielectric rods with radius $0.18a$ and dielectric constant $\epsilon = 11.56$, where $a = 0.5 \mu\text{m}$ is the lattice unit. These rods are shown by open circles. The defect shown by open bold gray circle has the radius $0.18a$ and $\epsilon_0 = 30$. Dashed open circles mark those rods whose removal fabricates the 1D PhC waveguide.

circles. As a result, we obtain the directional PhC waveguide that holds the nonlinear defect rod named as the dipole defect. Note after opening the dipole, eigenmodes cease to be solutions of the Maxwell equations and will decay into the arms of the waveguide. The principal role of the dipole modes for cross talking in the X-shaped waveguide and for the optical transistor was shown first in Refs. 13 and 29.

Therefore we can write for the electric field in the interior of the defect cavity,³⁰

$$E(x, y) = A_1 E_1(x, y) + A_2 E_2(x, y) + \tilde{\psi}(x, y), \quad (1)$$

where the complex background function $\tilde{\psi}$ is a small contribution of other nonresonant defect modes (monopole, quadrupole, etc.). Next, we assume that the cavity defect rod is made from a Kerr medium. Then, following the perturbation theory developed in Refs. 12 and 17, we write the following coupled-mode theory (CMT) equations for the amplitudes $A_m, m = 1, 2$:

$$\begin{aligned} [\omega - \omega_0 - V_{11} + i\gamma_1]A_1 - V_{12}A_2 &= i\sqrt{\gamma_1}E_{\text{in}}, \\ -V_{12}A_1 + [\omega - \omega_0 - V_{22}]A_2 &= 0, \end{aligned} \quad (2)$$

where

$$\langle m|V|n\rangle = -\frac{(\omega_m + \omega_n)}{4N_m} \int d^2\vec{r} \delta\epsilon(\vec{r}) E_m(\vec{r}) E_n(\vec{r}). \quad (3)$$

$$\delta\epsilon(\vec{r}) = \frac{n_0 c n_2 |E(\vec{r})|^2}{4\pi} \approx \frac{n_0 c n_2 |A_1 E_1(\vec{r}) + A_2 E_2(\vec{r})|^2}{4\pi} \quad (4)$$

is the nonlinear contribution to the dielectric constant of the defect rod with instantaneous Kerr nonlinearity, $n_0 = \sqrt{\epsilon_0}$ and n_2 are the linear and nonlinear refractive indexes, respectively, of the defect rod, c is the light velocity. Equation (4) instantly implies the normalization of the eigenmodes as follows:³¹

$$N_m = \int d^2\vec{r} \epsilon_{\text{PhC}} E_m^2(\vec{r}) = \frac{a^2}{c n_2}, \quad (5)$$

where ϵ_{PhC} is the dielectric constant of whole defectless PhC. Because of symmetry, $N_1 = N_2$. After substitution of Eqs. (3) and (5) into Eq. (2), we can write CMT equations in the dimensionless form

$$\begin{aligned} [\omega - \omega_0 + \lambda_{11}|A_1|^2 + \lambda_{12}|A_2|^2 + i\gamma_1]A_1 \\ + 2\lambda_{12}\text{Re}(A_1^* A_2)A_2 = i\sqrt{\gamma_1}E_{\text{in}}, \end{aligned}$$

$$\begin{aligned} 2\lambda_{12}\text{Re}(A_1^* A_2)A_1 + [\omega - \omega_0 + \lambda_{22}|A_2|^2 \\ + \lambda_{12}|A_1|^2]A_2 = 0, \end{aligned} \quad (6)$$

where E_{in} is the amplitude of light injected into the left side of the waveguide. Here, the frequencies, the width γ_1 , and the nonlinear constants are given in terms of $2\pi c/a$. One can see that if there is a solution (A_1, A_2) there is also the solution $(A_1, -A_2)$. With accuracy of notations Eqs. (6) coincides with the coupled-mode equations given in Ref. 13. We take the Kerr nonlinear refractive index $n_2 = 2 \times 10^{-12} \text{ cm}^2/\text{W}$. Other material parameters are listed in figure caption of Fig. 1. Then we obtain from Eqs. (3) and (5) $\lambda_{11} = \lambda_{22} = 1.05 \times 10^{-3}$, $\lambda_{12} = 3.36 \times 10^{-4}$, and $\gamma_1 = 7.5 \times 10^{-4}$.

The self-consistent solutions of Eq. (6) are presented in Fig. 2. We have found numerically, at least, three types of solutions. For the first, symmetry preserving solution shown in Fig. 2(a) by dashed blue lines, only the even dipole mode $E_1(x, y)$ is excited. Respectively, the transmission amplitude³² $t = \sqrt{\gamma_1}A_1$ has resonance behavior typical for the transmission in the waveguide coupled with the nonlinear in-channel defect with a single mode^{13-15,17} as shown in Fig. 2(c). For the second solution, the odd dipole mode is excited too for the frequency below some threshold, as shown in Fig. 2(b) by a solid gray line, because of nonlinear coupling of the dipole modes in Eq. (6). Then the contribution from the odd mode $E_2(x, y)$ to the light transmission $t = \sqrt{\gamma_1}A_1 + \sqrt{\gamma_2}A_2$ breaks the symmetry with respect to the center line of the waveguide. From the second equation in Eq. (6), we obtain that the phases of the complex amplitudes A_1 and A_2 coincide.

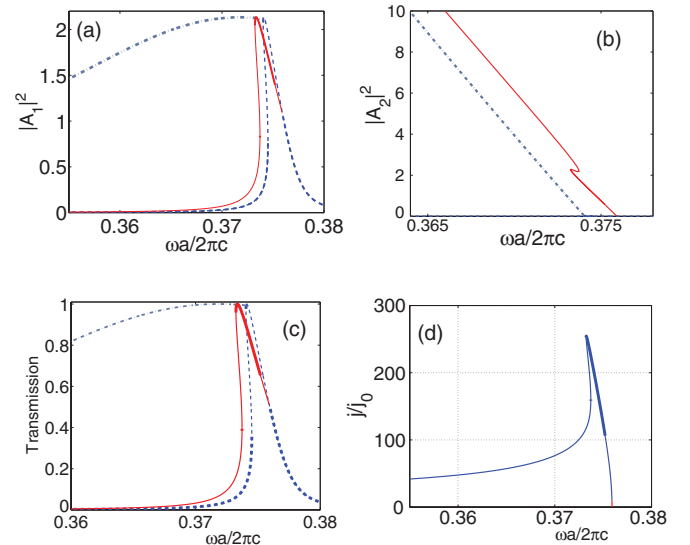


FIG. 2. (Color online) Frequency behavior of (a) intensity of the first even dipole mode, (b) intensity of the second odd dipole mode, (c) transmission, and (d) ratio of maximal value of the power current interior of the defect rod to the input PV $j_0 = P/a$ for $E_{\text{in}} = 0.04$. The last value corresponds to the input power per length $P = 1 \text{ W}/a$. Blue dashed lines show the symmetry preserving solution, gray dash-dotted lines show the symmetry breaking solution, and red solid lines show the phase symmetry breaking solution. In (c) and (d), thicker lines mark the stable solutions.

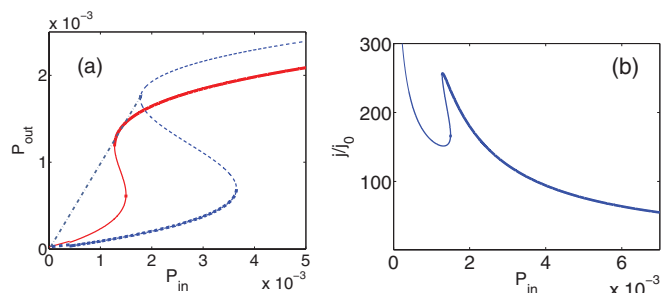


FIG. 3. (Color online) (a) Output power $P_{\text{out}} = \gamma_1 |A_1|^2$ and (b) ratio of maximal value of the PV current in the interior of the defect rod to the input PV current vs input power $P_{\text{in}} = |E_{\text{in}}|^2$ for $\omega = 0.3738$. Blue dashed line shows the symmetry preserving solution, gray dash-dotted line shows the symmetry breaking solution, and red solid line shows the phase symmetry breaking solution. Thicker lines mark the stable solutions.

Both symmetry preserving and symmetry breaking solutions exist provided that the determinant

$$\begin{vmatrix} \omega - \omega_0 + \lambda_{11}I_1 + \lambda_{12}I_2 + i\gamma_1 & 2\lambda_{12}\sqrt{I_1I_2}\cos\theta \\ 2\lambda_{12}\sqrt{I_1I_2}\cos\theta & \omega - \omega_0 + \lambda_{22}I_2 + \lambda_{12}I_1 \end{vmatrix} \quad (7)$$

does not equal zero. Here, we introduced the intensities $I_j = |A_j|^2$ and phase difference θ between the dipole modes amplitudes. However, there might be a special solution if determinant (7) equals zero.¹² Then, we easily obtain that $\theta = \pi/2$ or $\theta = 3\pi/2$ and the intensities of the dipole modes follow each other:

$$\lambda_{11}I_2 + \lambda_{12}I_1 = \omega_0 - \omega. \quad (8)$$

We define this special solution as a phase symmetry breaking solution. This solution exists for $\omega < \omega_0 = 0.3763$. Moreover, a substitution of Eq. (8) into Eq. (6) shows that the even dipole mode behaves as a single nonlinear mode coupled with injecting light:

$$[(\omega - \omega_0 + \Lambda I_1 + i\Gamma_1)A_1 = i\sqrt{\Gamma_1}\tilde{E}_{\text{in}}, \quad (9)$$

similar to the symmetry preserving solution, however, with the modified parameters, the effective nonlinear constant $\Lambda = \lambda_{11} + \lambda_{12}$, the effective resonance width $\Gamma_1 = \frac{\lambda_{11}}{\lambda_{11} - \lambda_{12}}\gamma_1$, and the effective injected amplitude $\tilde{E}_{\text{in}} = \sqrt{\frac{\lambda_{11}}{\lambda_{11} - \lambda_{12}}}E_{\text{in}}$. Hence the resonance behavior of the first dipole mode for the phase symmetry breaking solution differs from the symmetry preserving solution as seen from Fig. 2(a). Because of linear relation between the transmission amplitude and the first even dipole mode amplitude $t = \sqrt{\gamma_1}A_1$, the transmission completely follows I_1 as shown in Fig. 2(c). Furthermore, we studied the stability of solutions by standard methods given in Refs. 33 and 34 to show the stability domains by thicker lines in Fig. 2(c). The series of figures showing the frequency behavior of the dipole mode intensities and the transmission is supplemented with Fig. 3 where the input-output curves are shown for fixed frequency. It is interesting that the symmetry breaking solution results in a linear behavior of the input-output curve, however, it is not stable. One can see from Fig. 3(a) that the domains of

stability for the symmetry preserving solution and for the phase symmetry preserving solution are overlapped for the input power.

Let us consider now the PV of power current $\mathbf{j} = \frac{c^2}{8\pi\Omega}\text{Im}(E^*\nabla E)$. Here, all quantities are dimensional. Substituting $E \rightarrow \sqrt{cn_2}E$, $\omega = \Omega a/2\pi c$, and $\nabla \rightarrow a\nabla$, we introduce the dimensionless ratio of the PV,

$$\frac{j}{j_0} = \frac{1}{8\pi^2\omega|E_{\text{in}}|^2}\text{Im}(E^*\nabla E), \quad (10)$$

where $j_0 = P/a$, $P = \frac{a|E_{\text{in}}|^2}{2n_2}$. Here, j_0 is the input PV in the PhC waveguide. For the symmetry preserving solution, we have resonance excitation of the first even mode only. Substituting Eq. (1) with the first even dipole eigenmode as $E_1(x, y) = xf(r)$ into Eq. (10), we obtain that the power current within the defect rod is laminar, directed along the waveguide x and proportional to $|\tilde{\psi}|$, and therefore is small. As was evaluated in Ref. 35, the input and output currents are also proportional to $|\tilde{\psi}|$ that gives us the ratio $j/j_0 \sim 1$. For the symmetry breaking solution, both dipole modes are excited with the same phase. Therefore these amplitudes A_1 and A_2 can be considered as real, and the light amplitude in the interior of the defect can be written as $E(x, y) = (A_1x + A_2y)f(r) + \tilde{\psi}$. Respectively, we obtain that the power current in the interior of the defect has the same laminar behavior as for the symmetry preserving solution, however, the PV is tilted by the angle $\tan\phi = (I_2/I_1)^{1/2}$ relative to the transport axis.

For the phase symmetry breaking solution, we obtain $E(x, y) = (\sqrt{I_1}x + \sqrt{I_2}iy)f(r) + \tilde{\psi}$. Then the PV current $\mathbf{j} \sim \text{Im}(A_1A_2^*)f^2(r)(y, -x) = \sqrt{I_1I_2}f^2(r)(y, -x)$ where the small contribution of the background function $\tilde{\psi}$ can be neglected. One can see that the PV circulates around the center of the defect and substantially exceeds the input PV as we show below. Let us evaluate the PV within the defect given by $\sqrt{I_1I_2}$. Figure 2(a) shows that the first dipole mode I_1 demonstrates typical resonance behavior, and then rapidly decays beyond the resonance width as it occurs for the other solutions. However, the intensity I_2 linearly grows as the frequency is decreased [see Fig. 2(b)]. As a result, the frequency behavior of the value $\sqrt{I_1I_2}$ is rather large in a wide frequency region as seen from Fig. 2(d). Moreover, there is a resonant contribution of the intensity I_1 . From Eqs. (8) and (9), one can evaluate the maximal values of the intensities $I_1 = I_2 = \frac{1}{\gamma_1} \frac{\lambda_{11} - \lambda_{12}}{\lambda_{11}} E_{\text{in}}^2$ at the resonance frequency that defines the maximal PV. Since the input current is proportional to E_{in}^2 , we obtain another important result that the ratio of the inner PV to the input PV is given by the inverse of the coupling constant of the even dipole mode γ_1 . There is also the equivalent phase symmetry breaking solution with the phase difference $\theta = 3\pi/2$, which gives rise to the giant Optical vortex (OV) with opposite circulation. Figure 3(b) shows how the power current behaves with the growth of input power for fixed frequency. We show that the giant OV is stable for the input power exceeding the threshold one. The peak in the PV is due to a bistability of the phase symmetry breaking solution as seen from Fig. 3(a). Typically, there might be bifurcations from one stable phase symmetry breaking solution with the phase difference $\pi/2$ and positive vorticity to the second equivalent stable solution with the phase difference $3\pi/2$ and negative vorticity. However,

as seen from Fig. 3(a), there is also the bifurcation from the stable symmetry preserving solution with no OV to the stable phase symmetry breaking solution with $\theta = \pi/2$ and the OV with positive vorticity or to the solution with $\theta = 3\pi/2$ with negative vorticity.

III. SOLUTIONS IN PHOTONIC CRYSTAL

The above comprehensive considerations are in full agreement with numerical computations of the light amplitude by use of the Maxwell equations with an optical nonlinear defect rod shown in Fig. 4. For the symmetry preserving solution, Fig. 4(a) demonstrates that the even dipole mode is excited only. Optical streamlines of the PV are almost parallel to the waveguide. For the symmetry breaking solution, Fig. 4(c) shows that the symmetrical light transmitting through the waveguide excites both dipole modes to give rise to the breaking of the center line mirror symmetry. As a result, the light streamlines tilt in the interior of the defect cavity. The nodal lines of $\text{Re}(\psi)$ and $\text{Im}(\psi)$ coincide within the cavity that means we have no optical vortex there. Respectively, we

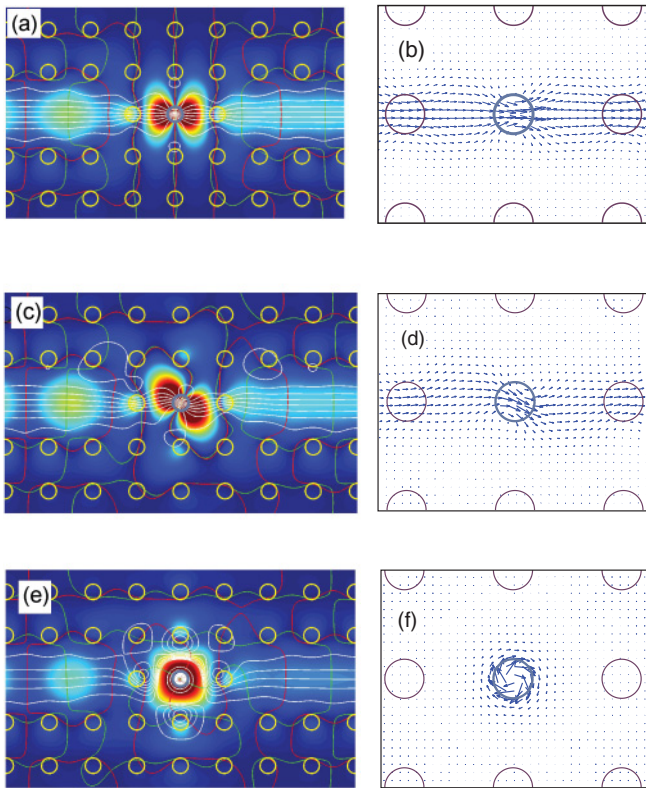


FIG. 4. (Color online) Absolute value of light amplitude (electric field) and optical streamlines in the PhC waveguide with a single nonlinear defect shown by the thick gray open circle for $a\omega/2\pi c = 0.3722$, $P = 1W/a$. Rods of the PhC are shown by open circles. Light incident at the right side of the PhC waveguide transmits through the in-channel nonlinear defect rod cavity presented by two dipole modes shown in Fig. 1. Green and red solid lines show nodal lines of real and imaginary parts of the wave function. White solid lines show light streamlines. (b), (d), and (f) show the PV of power current. (a) and (b) symmetry preserving solution, (c) and (d) symmetry breaking solution, and (e) and (f) phase symmetry breaking solution.

have the laminar PV streamlines tilted in the interior of defect cavity as shown in Fig. 4(d).

At last, for the phase symmetry breaking solution, Fig. 4(e) shows that the nodal line of $\text{Re}(\psi)$ crosses the nodal line of $\text{Im}(\psi)$ at the center of the defect rod by the angle $\pi/2$ to give rise to an optical vortex as shown in Fig. 4(f). The absolute value of the light amplitude is fully symmetric relative to the center line. Nevertheless, the symmetry is broken because of the energy flow, which is vortical around the defect rod with the vorticity $\mathbf{v} = \nabla \times \mathbf{j}$ directed down. There is also the fully equivalent phase symmetry breaking solution with the vorticity directed up, which is not shown in Fig. 4. Moreover, we present the frequency behavior of the light transmission and the maximal value of the power current within the defect rod shown in Fig. 5. Comparison with Fig. 2 demonstrates excellent agreement with the CMT-based calculations besides the symmetry breaking solution. That is not surprising because the CMT parameters were obtained for the specific PhC structure shown in Fig. 1. The small difference between the CMT transmission in Fig. 2(c) and the transmission in PhC structure shown in Fig. 5(a) is the result of, presumably, the radiation shift of the eigendipole modes.

IV. SHIFTED DEFECT IN WAVEGUIDE

The value of the PV energy flow in optical vortex can be taken extremely large by diminishing of the coupling constant γ_1 . That can be achieved by “hiding” of the defect rod among the linear defect rods. For the configuration shown in Fig. 4, the value of the PV around the defect rod is roughly 200 times more than the incident power current resulted in a giant optical vortex. Optical vortices predicted long time ago by Nye and Berry¹⁸ were observed in many experiments³⁶ as wave-front dislocations in interference patterns of beams (holograms). However, the transmission properties do not depend on the sign of the vorticity of the optical vortex. We propose a scheme in which the transmission is directly related to the vorticity.^{37,38} Following Refs. 5 and 26, we apply light to the left and right sides of the waveguide with equal intensity and equal phase. However, we shift the defect rod relative to the center line of the waveguide by a magnitude $0.3a$ as shown in Fig. 6. That system does not preserve the center line mirror symmetry

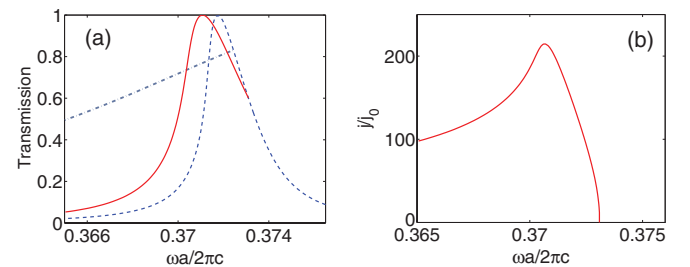


FIG. 5. (Color online) Frequency behavior of (a) the light transmission and (b) ratio of maximal value of the PV power current interior of the defect rod to the input current $j_0 = P/a$ for $P = 1W/a$ obtained from the Maxwell equations. Blue dashed line shows the symmetry preserving solution, gray dash-dotted line shows the symmetry breaking solution, and red solid line shows the phase symmetry breaking solution.

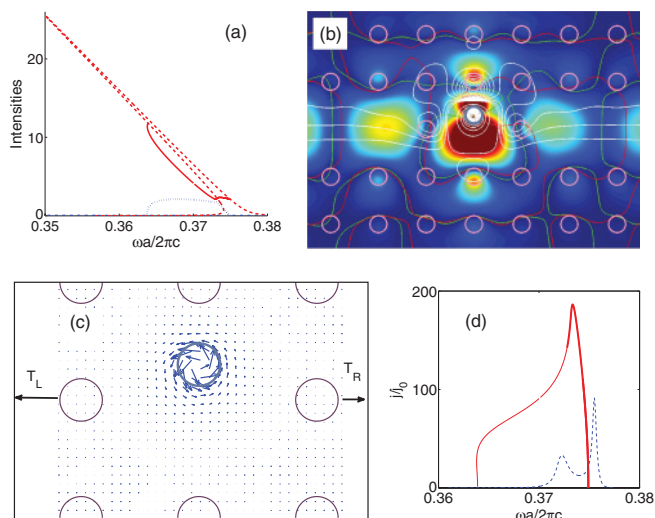


FIG. 6. (Color online) Light with the same amplitude is applied to both sides of PhC waveguide. (a) Frequency behavior of the light intensities of the dipole modes. Dashed/solid red lines show the intensity of the even dipole mode even relative to left and right reflection for the symmetry preserving/symmetry breaking solutions. Dash-dotted/dotted lines show the intensity of the odd dipole mode for the symmetry preserving/symmetry breaking solutions. (b) Absolute value of light amplitude and light streamlines in the PhC waveguide with a shifted nonlinear defect shown by the thick gray open circle for $E_{in} = 0.04$. (c) PV currents of energy in the vicinity of the nonlinear defect rod. (d) Ratio of maximal value of the PV in the interior of the defect rod to the input PV.

but does have the left-right mirror symmetry with respect to cross-sectional axis. If the nonlinear defect is presented by two dipole resonance modes, then the symmetry breaking gives rise to the difference of light outputs from the waveguide:

$$t_{L,R} = -E_{in} + \sqrt{\gamma_1}A_1 \pm \sqrt{\gamma_2}A_2. \quad (11)$$

As we show below, that difference is strictly related to the direction of current circulation around the defect, i.e., to the vorticity of the OV.

Similar to Eq. (6), we have the following CMT equations:

$$\begin{aligned} [\omega - \omega_1 + \lambda_{11}|A_1|^2 + \lambda_{12}|A_2|^2 + i\gamma_1]A_1 \\ + 2\lambda_{12}\text{Re}(A_1^*A_2)A_2 = 0, \\ 2\lambda_{12}\text{Re}(A_1^*A_2)A_1 + [\omega - \omega_2 + \lambda_{22}|A_2|^2 \\ + \lambda_{12}|A_1|^2 + i\gamma_2]A_2 = 2i\sqrt{\gamma_2}E_{in}, \end{aligned} \quad (12)$$

where for the PhC structure parameters are the following $\omega_1 = 0.3722$, $\omega_2 = 0.3756$, $\gamma_1 = 0.0007$, $\gamma_2 = 0.00025$, $\lambda_{11} = 0.001$, $\lambda_{22} = 0.00094$, and $\lambda_{12} = 0.0003$.

There are two types of self-consistent solutions of Eq. (12), symmetry preserving and symmetry breaking solutions, but there is no phase symmetry breaking solution as shown in Fig. 6(a). In Fig. 6(c), the wave function for the electric field calculated from the Maxwell equations is shown for the symmetry breaking solution. One can see that the light intensities at the waveguide sides are different. However, the optical streamlines preserve the mirror symmetry. Only direction of the PV, and, respectively, the vorticity of OV

are related to the difference between the light outputs $T_L = 0.806$ and $T_R = 0.19$ as shown in Fig. 6(d). There is also the equivalent symmetry breaking solution with the vorticity directed down with the transmissions $T_L = 0.19$ and $T_R = 0.806$. Therefore we observe that the light outputs correlate with the vorticity of optical vortex.

For the shifted linear defect rod with two dipole eigenmodes, we have the OV provided that light is injected from the one side of waveguide. That OV might be giant too if the dipole modes are weakly coupled with the waveguide as shown in Fig. 6(b) by the thin line. However, in contrast with the nonlinear case, the price for it is that the OV can be considered as giant at resonant frequencies only as seen from Fig. 6(b). Moreover, the ratio j/j_0 does not depend on the intensity of injected light in contrast to the symmetry breaking solution.

V. SUMMARIES AND CONCLUSIONS

Previously, as it was summarized in the introduction, a system of at least two nonlinear defects with single monopole resonance modes was used to realize the symmetry breaking in waveguides.^{5,12} In the present paper, we reported that the phenomenon of symmetry breaking can be achieved in a single nonlinear dipole defect. Apparently, such a system is the simplest optical circuit where the symmetry breaking could take place. We show that the mirror reflection symmetry of the system can be broken either by light intensity or light phase. For the last scenario of symmetry breaking, incident light excites both dipole modes $xf(r)$ and $yf(r)$ with phase difference $\pi/2$ or $3\pi/2$ to give rise to the total defect state as $(\sqrt{T_1}x \pm i\sqrt{T_2}y)f(r)$. As it was shown by Nye and Berry,¹⁸ that state holds a power current vortex with clockwise or counterclockwise circulation around the defect. The novelty of our result is that the OV is giant with the power current within the defect rod exceeding the power current in the waveguide by two orders of magnitude. That giant power current is mostly localized within the nonlinear defect as shown in Fig. 4(f). We emphasize that for a symmetrical position of the nonlinear defect rod, the OV exists only for the phase symmetry breaking solution, while for the symmetry preserving and for the symmetry breaking solutions, there are laminar flows as shown in Figs. 4(c) and 4(e). The stability domains of the symmetry preserving solution and of the phase symmetry preserving solution overlap, as shown in Fig. 3(a). Thus there might be an all-optical switching between these solutions with switching on/off the giant OV.

We also considered the PhC structure with the nonlinear defect rod shifted relative to the center line of the PhC directional waveguide. If light is injected to both sides of the waveguide with equal intensity and equal phase, the system is symmetric relative to mirror reflection with respect to the cross-sectional axis of the waveguide. Respectively, in the linear case, one would have equal light outputs, which agrees with the time-reversal symmetry. However, for the nonlinear defect, the light outputs may become different. This phenomenon was firstly found by Maes *et al.*^{5,26} for two nonlinear defects in the directional waveguide. The importance of our result for the nonlinear dipole defect is that the difference between the outputs is linked to the vorticity of the OV. For the symmetry breaking solution with the left output larger than

the right, the PV circulates around the defect counterclockwise as shown in Fig. 6(c). There is also an equivalent solution where the right output dominates with the PV circulating clockwise.

ACKNOWLEDGMENTS

The work is partially supported by RFBR grant 12-02-00483. We thank D. N. Maksimov and K.N. Pichugin for assistance in the manuscript preparation.

-
- ¹M. Haelterman and P. Mandel, *Opt. Lett.* **15**, 1412 (1990).
²T. Peschel, U. Peschel, and F. Lederer, *Phys. Rev. A* **50**, 5153 (1994).
³I. V. Babushkin, Yu. A. Logvin, and N. A. Loiko, *Quantum Electron.* **28**, 104 (1998).
⁴J. P. Torres, J. Boyce, and R. Y. Chiao, *Phys. Rev. Lett.* **83**, 4293 (1999).
⁵B. Maes, P. Bienstman, and R. Baets, *Opt. Express* **16**, 3069 (2008).
⁶K. Huybrechts, G. Morthier, and B. Maes, *J. Opt. Soc. Am. B* **27**, 708 (2010).
⁷N. Akhmediev and A. Ankiewicz, *Phys. Rev. Lett.* **70**, 2395 (1993).
⁸R. Tasgal and B. A. Malomed, *Phys. Scr.* **60**, 418 (1999).
⁹A. Gubeskys and B. A. Malomed, *Eur. Phys. J. D* **28**, 283 (2004).
¹⁰E. A. Ostrovskaya, Y. S. Kivshar, M. Lisak, B. Hall, F. Cattani, and D. Anderson, *Phys. Rev. A* **61**, 031601 (2000).
¹¹V. A. Brazhnyi and B. A. Malomed, *Phys. Rev. A* **83**, 053844 (2011).
¹²E. N. Bulgakov, K. N. Pichugin, and A. F. Sadreev, *J. Phys.: Condens. Matter* **23**, 065304 (2011); *Phys. Rev. B* **83**, 045109 (2011).
¹³M. F. Yanik, S. Fan, and M. Soljačić, *Appl. Phys. Lett.* **83**, 2739 (2003).
¹⁴A. R. McGurn, *Chaos* **13**, 754 (2003); *J. Phys.: Condens. Matter* **16**, S5243 (2004).
¹⁵A. E. Miroshnichenko, S. F. Mingaleev, S. Flach, and Yu. S. Kivshar, *Phys. Rev. E* **71**, 036626 (2005).
¹⁶J. Bravo-Abad, S. A. Rodriguez, P. Bermel, S. G. Johnson, J. D. Joannopoulos, and M. Soljačić, *Opt. Express* **15**, 16161 (2007).
¹⁷J. Joannopoulos, S. G. Johnson, J. N. Winn, and R. D. Meade, *Photonic Crystals: Molding the Flow of Light* (Princeton University Press, Princeton, NY, 2008).
¹⁸J. F. Nye and M. V. Berry, *Proc. R. Soc. London* **336**, 165 (1974).
¹⁹A. A. Maier, *Sov. J. Quantum Electron.* **12**, 1940 (1982).
²⁰H. M. Gibbs, *Optical Bistability: Controlling Light with Light* (Academic, New York, 1985).
²¹S. M. Jensen, *IEEE J. Quantum Electron.* **18**, 1580 (1982).
²²S. R. Friberg, Y. Silberberg, M. K. Oliver, M. J. Andrejco, M. A. Saifi, and P. W. Smith, *Appl. Phys. Lett.* **52**, 1135 (1987).
²³Y. Chen, A. W. Snyder, and D. N. Payne, *IEEE J. Quantum Electron.* **28**, 239 (1992).
²⁴N. Boumaza, T. Benouaz, A. Chikhaoui, and A. Cheknane, *Int. J. Phys. Sci.* **4**, 505 (2009).
²⁵V. Grigoriev and F. Biancalana, *Opt. Lett.* **36**, 2131 (2011).
²⁶B. Maes, M. Soljačić, J. D. Joannopoulos, P. Bienstman, R. Baets, S.-P. Gorza, and M. Haelterman, *Opt. Express* **14**, 10678 (2006).
²⁷E. N. Bulgakov and A. F. Sadreev, *Phys. Rev. B* **84**, 155304 (2011).
²⁸K. Busch, S. F. Mingaleev, A. Garcia-Martin, M. Schillinger, and D. Hermann, *J. Phys.: Condens. Matter* **15**, R1233 (2003).
²⁹S. G. Johnson, C. Manolatou, S. Fan, P. R. Villeneuve, J. D. Joannopoulos, and H. A. Haus, *Opt. Lett.* **23**, 1855 (1998).
³⁰A. F. Sadreev, *Phys. Rev. E* **70**, 016208 (2004).
³¹M. Soljačić, C. Luo, J. D. Joannopoulos, and S. Fan, *Opt. Lett.* **28**, 637 (2003).
³²W. Suh, Z. Wang, and S. Fan, *IEEE J. Quantum Electron.* **40**, 1511 (2004).
³³N. M. Litchinitser, C. J. McKinstrie, C. M. deSterke, and G. P. Agrawal, *J. Opt. Soc. Am. B* **18**, 45 (2001).
³⁴A. R. Cowan and J. F. Young, *Phys. Rev. E* **68**, 046606 (2003).
³⁵A. F. Sadreev and K.-F. Berggren, *Phys. Rev. E* **70**, 026201 (2004).
³⁶G. Popescu and A. Dogariu, *Phys. Rev. Lett.* **88**, 183902 (2002); J. Leach and M. J. Padgett, *New J. Phys.* **5**, 154 (2003); Y. F. Chen, T. H. Lu, and K. F. Huang, *Phys. Rev. Lett.* **96**, 033901 (2006); J. Courtial and K. O'Holleran, *Eur. Phys. J. Special Topics* **145**, 35 (2007); A. V. Carpentier, H. Michinel, J. R. Salgueiro, and D. Olivieri, *Am. J. Phys.* **78**, 916 (2008).
³⁷M. Berry and M. R. Dennis, *Proc. R. Soc. London A* **456**, 2059 (2000).
³⁸A. I. Saichev, K.-F. Berggren, and A. F. Sadreev, *Phys. Rev. E* **64**, 036222 (2001).